HYDROLOGICAL PROCESSES
Hydrol. Process. (2009)
Published online in Wiley InterScience
(www.interscience.wiley.com) DOI: 10.1002/hyp.7353

Simulation of *Populus euphratica* root uptake of groundwater in an arid woodland of the Ejina Basin, China

Yonghua Zhu,[1,2]* Liliang Ren,[1] Todd H. Skaggs,[2] Haishen Lü,[1,3] Zhongbo Yu,[1,4] Yanqing Wu[5] and Xiuqin Fang[1]

[1] *State Key Laboratory of Hydrology-Water Resources and Hydraulic Engineering, Hohai University, Nanjing, 210098, China*
[2] *U.S. Salinity Laboratory, 450 W. Big Springs Rd., Riverside, CA, 92507, USA*
[3] *College of Science, Hohai University, Nanjing, 210098, China*
[4] *Department of Geoscience, University of Nevada, Las Vegas, NV 89154, USA*
[5] *School of Environmental Science and Engineering, Shanghai Jiaotong University, Shanghai 200240, China*

Abstract:

The Ejina Basin is an extremely arid subwatershed in Northwest China. The predominant natural tree species in the area, *Populus euphratica*, depends on groundwater for sustenance. In recent decades, groundwater overdraft and increased water diversions from the Heihe River caused water table elevations to decline, such that large areas of *P. euphratica* have withered, creating a highly visible symbol of ecological change and desertification in the Ejina Basin. Ecological restoration efforts aimed at saving existing woodlands and cultivating new stands of *P. euphratica* are underway. To provide a better scientific basis for ecological restoration plans, it is necessary to understand the effect of water table elevation on *P. euphratica* water uptake. In this work, we used the HYDRUS-1D software package to study groundwater movement into the root zone and the uptake of groundwater in a 10-year-old *P. euphratica* woodland. Additionally, we examined the changes in uptake that would occur for different water table elevations. The model calibration was confirmed by comparing predicted soil moisture contents during the *P. euphratica* growing season with field measured values. The results indicate that in 2000, with an average water table depth of 2·64 m, *P. euphratica* at the study site obtained about 53% of its water from groundwater during the middle part of the growing season (day of year 160–290). Simulations made with constant water table depths found that increasing the water table depth from 2 to 3 metres resulted in a 74% reduction in transpiration. Many factors can influence the optimal water table depth at a given site. An advantage of the modelling approach is that these factors can be systematically varied, creating a site-specific impact assessment of water management options that may alter water table depths, thus aiding ecological restoration efforts. Copyright © 2009 John Wiley & Sons, Ltd.

KEY WORDS arid region; HYDRUS-1D; *P. euphratica*; root water uptake; shallow groundwater

Received 30 July 2008; Accepted 5 April 2009

INTRODUCTION

The Ejina Basin in Northwest China is an extremely arid region that contains the lower reaches of the Heihe River, the second longest inland river in China. The region has a harsh continental climate with an average temperature of 8 °C, a maximum of 41 °C (July) and a minimum of −36 °C (January). Because annual precipitation is only 38 mm, vegetation in the Ejina Basin, notably riparian woodlands along the Heihe and natural oases near the boundary of the Gobi and Badanjilin deserts, depends heavily on groundwater for sustenance. Consequently, when groundwater levels in the Ejina Basin declined during the latter part of the 20th century due to groundwater overdraft and increased use of river water for irrigation in the middle reaches of the Heihe (Wang and Chen, 1999; Chen *et al.*, 2005; Qi and Cai, 2007; Qi and Luo, 2007), a substantial die-off of vegetation occurred, with dire consequences. The Ejina Oasis plays a protective role, blocking winds and stabilizing sands. The withering of the oasis led to increased sandstorms in Northwest and Northern China (Du *et al.*, 2005; He and Zhao, 2006), including an unprecedented heavy sandstorm in the spring of 2000 that created economic and health problems in areas as far away as Beijing and Tianjin (Xu *et al.*, 2003). If the Ejina Oasis disappears completely, the consequences could be devastating. Ongoing efforts to restore and improve basin ecology are critically important and cannot be delayed (Qi and Luo, 2007).

The dominant natural tree species in the Ejina Basin is *Populus euphratica*, a deciduous poplar tree with high drought and salinity tolerances (Gu *et al.*, 2004; Yang *et al.*, 2007). In recent decades, large areas of *P. euphratica* have withered, creating a highly visible symbol of ecological change and desertification in the Ejina Basin. In the 1950s, 50 000 ha of *P. euphratica* existed, whereas in 1998, only 22 667 ha were left (Bai *et al.*, 2008). By 2004, some restoration had occurred, although the area of *P. euphratica* was still only 38 663 ha (Lu *et al.*, 2007).

Given the low level of precipitation, a fundamental aspect of Ejina Basin eco-hydrology is the movement

* Correspondence to: Yonghua Zhu, State Key Laboratory of Hydrology-Water Resources and Hydraulic Engineering, Hohai University, Nanjing, 210098, China. E-mail: Yonghua321@yahoo.com.cn

of groundwater into the root zone and the uptake of that water by plants. Understanding and quantifying this water flux in *P. euphratica* woodlands is crucial to improving ecological restoration efforts.

Past research on the contribution of groundwater to plant uptake has been performed for a number of different environments, including several studies focusing on row crops and grasses (e.g. Ayars and Schoneman, 1986; Soppe and Ayars, 2003; Kahlown *et al.*, 2005; Babajimopoulos *et al.*, 2007). Research focusing specifically on *P. euphratica* woodlands in China includes a number of studies that measured physiological stress in trees as a function of groundwater elevation (Chen YN *et al.*, 2004; Chen YP *et al.*, 2006; Zhuang and Chen, 2006), although most of these studies were conducted in the Tarim River basin rather than the Heihe River basin. Also, these studies were mainly empirical and did not examine in detail the physical mechanisms involved in the uptake of groundwater. In the Heihe River basin, Yan *et al.* (2005) used Geographic Information System (GIS) and numerical simulation techniques to analyse the influence of groundwater depth on vegetation coverage in various plant communities (grassland, shrub, woodland and forest), while Cao *et al.* (2004) and Si *et al.* (2005) reported observations of general ecosystem recovery following changes in water management that increased water flow into the basin. Again, however, these studies did not evaluate mechanistically the uptake of ground water by *P. euphratica.*

Babajimopoulos *et al.* (2007) note that most previous research on groundwater contributions has been conducted using weighing and drainage lysimetres. This method is accurate but it is limited by relatively high construction, operation and maintenance costs. Babajimopoulos *et al.* (2007) therefore proposed estimating the contribution of groundwater using the mathematical model SWBACROS (Babajimopoulos *et al.*, 1995). We have adopted a similar approach in the present research.

Our objective was to estimate the contribution of groundwater to root zone soil moisture and root uptake in a *P. euphratica* woodland using the HYDRUS-1D software package (Šimůnek *et al.*, 2005). HYDRUS-1D is a well-known mechanistic model for simulating variably saturated water flow and root water uptake in soils. In this work, we first compare HYDRUS-1D simulations of root zone soil moisture with field measurements made in a *P. euphratica* woodland to verify that HYDRUS-1D is suitable for this application. Then, we use the model to estimate the contributions of groundwater to root water uptake and investigate the effect of groundwater depth on uptake.

MATERIALS AND METHODS

Field site

Our work is based on data gathered at a Chinese Academy of Sciences eco-hydrological research site (41°57′N, 101°20′E and 940·5 m above sea level) located in a riparian woodland in the Ejina Basin, 4 km southwest of Ejina City. The site is near the northwestern edge of the Badanjilin desert, in the lower reaches of the Heihe River basin (Figure 1). The region possess a continental climate with mean annual precipitation of 38 mm, mean annual free water surface evaporation of 3632 mm and mean temperature of 8 °C (Zhu, 2002; Zhu and Wu, 2003). The *P. euphratica* trees at the research site are 10 years old and have not been significantly affected by human activities other than the site being fenced on its perimetre. The research site is located 450 m from the river, has an area of 1430 m^2 and an average tree density of 1 tree per 15 m^2. The topography is flat. At the time of the study in 2000, the average tree crown was 185 cm × 140 cm, the average height was 265 cm and the surface coverage of *P. euphratica* was 55%.

Field study

The study area was divided into five equal subplots. From each subplot, one tree with average height and tree crown characteristics was selected for growth measurements. A branch from each of the top, middle and bottom crown layers was chosen to measure growth. The branch length was measured once every 15 days. At the same time, leaf area index (LAI) on the selected trees was measured with a LAI-2000 Plant Canopy Analyzer (LI-COR, USA). LAI readings were taken from the four cardinal directions around the base of each tree using one sensor with a 90° view cap. Readings were taken along side the canopy (background measurement) as well as beneath the canopy. Measurements were made near sunset.

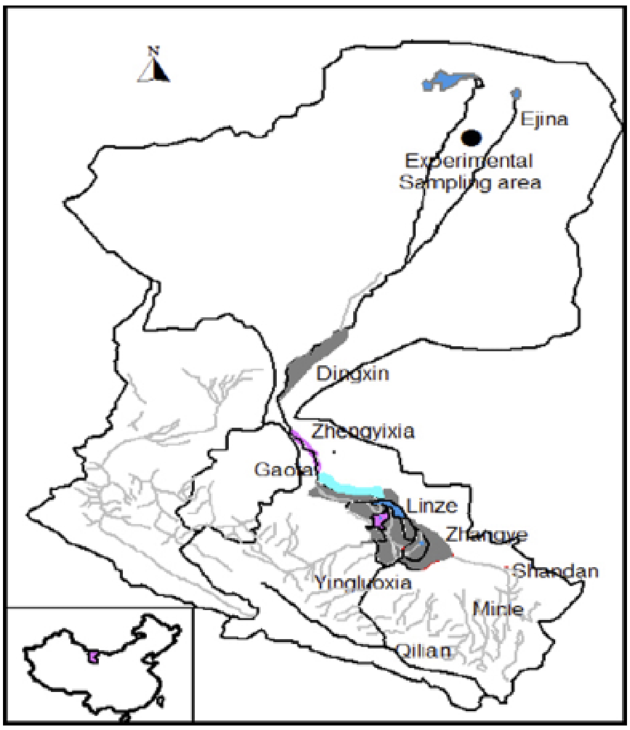

Figure 1. Location of the experimental site

DOI: 10.1002/hyp

Within each of the five subplots, a site was chosen to monitor soil moisture. The selected sites had soil characteristics that were representative of the subplots. Measurements were made every 5 days throughout the period 1st May to 31st October, 2000. On these days, a soil core measuring 200 cm long and 2·5 cm in diameter was extracted with a soil sampler and sectioned into 11 layers: 0–10, 10–20, 20–40, 40–60, 60–80, 80–100, 100–120, 120–140, 140–160, 160–180 and 180–200 cm. Three replicate samples were taken near the midpoint of each layer. The samples were weighed as collected, dried overnight at 105 °C and then re-weighed to determine by difference the mass of water in the soil sample. These gravimetric moisture contents were converted to volumetric contents using a soil bulk density value of 1·4 g cm^{-3} as reported for the field site by Feng and Chen (1999). The branch length, LAI and soil moisture data from the five subplots were averaged to obtain single values of these data the entire field site. The canopy data were used in the calculation of potential evapotranspiration rates, as discussed below.

Measurements of the effective root length distribution were taken on 15th August, 2000. One tree was selected in the study area. The soil and roots beneath this tree were excavated in 20 cm layers to a depth of 2·6 m and a radial distance of 1·75 m. The roots in each layer were separated from the soil and their diameters and lengths measured. All roots with diameter less than 10 mm were classified as effective roots, active in absorbing water from the soil (Zhu, 2002). Roots were found to be distributed throughout the soil profile to a depth of 200 cm, with the highest concentration of roots being in the 60–100 cm layer. The active root distribution is described in greater detail below.

The soil texture in the study area is sand (91·2% sand, 4·8% silt and 4% clay). In some locations, a silty layer between 1·0 and 1·2 m exists in an otherwise homogenous profile; in our simulations and analysis, we treat the profile as being homogeneous.

Figure 2 shows the measured precipitation and the water table depth during the 2000 growth period for *P. euphratica* (May through October). The water table elevation was measured in one observation well located 40 m northeast of the study area. The depth ranged from 2 to 3 m, with an average depth of 2·64 m (Figure 2). Precipitation data and data needed for calculating potential evapotranspiration such as air density ρ_a and saturation vapour pressure e_s were obtained from the Ejina County Weather Station.

Simulations

HYDRUS-1D (Šimůnek *et al.*, 2005) was used to simulate water flow and root water uptake. This model simulates one-dimensional flow and uptake processes (in our case, in the vertical direction). In some instances, it is natural to approximate field-average behaviour with a one-dimensional model. For example, a grass field where variability in the horizontal plane is minimal might be modelled as one dimensional. In the *P. euphratica* woodland, flow and uptake processes are not one dimensional. Variability exists across the land surface due to the irregular spacing of trees and the presence of undershrubs between trees. Our one-dimensional simulations thus do not represent field average behaviour, but instead represent flow and uptake beneath a single, typical tree, with the one-dimensional root structure being an effective system that conceptually results from integrating any horizontal variability that exists in the actual root structure.

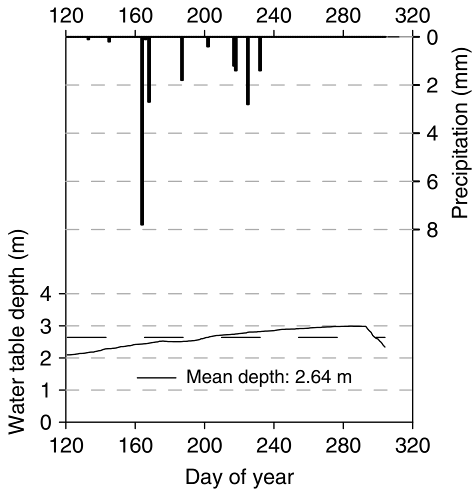

Figure 2. Time variation of precipitation and water table depth at the experimental site

In HYDRUS-1D, the governing water flow equation is the Richards equation with a sink term added to simulate the extraction of water by roots (Šimůnek *et al.*, 2005):

$$\frac{\partial \theta}{\partial t} = \frac{\partial}{\partial z}\left[k(h)\frac{\partial h}{\partial z} + k(h)\right] - S(z, t) \qquad (1)$$

where θ (cm^3 cm^{-3}) is the volumetric water content, h (cm) is the water pressure head, t (day) is time, z (cm) is the vertical space coordinate, k (cm day^{-1}) is the hydraulic conductivity and S (cm^3 cm^{-3} day^{-1}) is the sink term. The hydraulic conductivity k is represented using the van Genuchten-Mualem model:

$$S_e(h) = \frac{\theta(h) - \theta_r}{\theta_s - \theta_r} = \begin{cases} (1 + |\alpha_{vg} h|^n)^{-m} & h < 0 \\ 1 & h \geq 0 \end{cases} \qquad (2)$$

$$k(h) = k_s S_e^l [1 - (1 - S_e^{1/m})^m]^2 \qquad (3)$$

where S_e is the effective saturation, θ_s (cm^3 cm^{-3}) is the saturated water content, θ_r (cm^3 cm^{-3}) is the residual water content, k_s (cm day^{-1}) is the saturated hydraulic conductivity and n, m, α_{vg} (cm^{-1}) and l are adjustable parameters with $m = 1 - 1/n$.

The sink term is expressed as follows (e.g. Skaggs *et al.*, 2006a,b):

$$S(z, t) = T_p \; R(z) \; \alpha[h(z, t)] \qquad (4)$$

where T_p (cm^3 cm^{-2} day^{-1}) is the potential transpiration rate, $R(z)$ (cm^{-1}) is the relative root length distribution function and α ($0 \leq \alpha \leq 1$) is the dimensionless uptake

DOI: 10.1002/hyp

reduction function that accounts for decreases in uptake due to decreasing soil moisture content and is given by (van Genuchten, 1987; Skaggs *et al.*, 2006b):

$$\alpha(h) = \frac{1}{1 + (h/h_{50})^{\mathrm{p}}} \tag{5}$$

where h_{50} is the pressure head at which transpiration is halved and p is an adjustable constant that determines the steepness of the transition from potential to reduced uptake rates as h decreases. Introduced by van Genuchten (1987), Equation (5) is appropriate for environments where saturated or near-saturated soil conditions are not expected to exist for significant periods of time.

Equation (5) is an S-shaped function specifying that at a given depth in the root zone, uptake declines from the potential rate as the pressure head decreases. Typically, this decline is expected to occur over a range of several thousands of centimetres of pressure head (roots having been known under some conditions to extract water at pressure heads approaching −15 000 cm). Consistent with this expectation, parameter values reported in the literature for specific plants and soils range approximately from −1000 to −5000 cm for h_{50} and from 1·5 to 3 for p (Skaggs *et al.*, 2006a). However, with very coarse soil material such as the soil at the *P. euphratica* field site, the situation is different because the soil is almost completely drained of water at fairly modest pressure heads, say −300 or −400 cm. Using values for h_{50} and p that are similar to those reported in the literature cause the uptake reduction to operate essentially as a step function: When water is present in any appreciable amount, uptake at that depth is at (or very near) the potential rate, and switches rapidly to (effectively) zero when S_e approaches zero (Skaggs *et al.*, 2006a).

The parameter h_{50} may be viewed as an effective parameter that lumps together in some unspecified way the reduction in uptake due to reduced water potential at the root surface as well reduced flow of water to the root surface (Skaggs *et al.*, 2006a). On the basis of the latter consideration, an h_{50} value considerably lower than reported in the literature seems justifiable for very coarse soils. Likewise, a larger value of p could be required to account for the steepness of the soil water retention curve. However, Skaggs *et al.* (2006a) simulated root water uptake in sand and found that the step-like behaviour of the reduction function meant that the computed uptake was mostly insensitive to these parameter values, with the computed uptake being about the same for a range of parameter values. Nevertheless, Skaggs *et al.* (2006a) found the computed uptake to be in agreement with measured data. As discussed below in the Results section, we performed simulations using a range of values for h_{50} and p as part of an effort to calibrate HYDRUS-1D.

Boundary and initial conditions. The upper boundary was specified as an 'atmospheric' boundary condition (Šimůnek *et al.*, 2005). With an atmospheric boundary condition, potential evaporation and transpiration rates are specified by the user, in our case on a daily basis. The model then determines the actual evaporation and transpiration rates based on the simulated soil moisture conditions. In the case of evaporation, water evaporates from the soil surface at the potential rate (a flux boundary condition) whenever the pressure head at the surface is above a threshold value h_{crit}. If the soil surface dries out such that the surface pressure head reaches the threshold value, the boundary switches to a constant pressure head condition ($= h_{\mathrm{crit}}$), generally leading to a computed actual evaporation rate that is well below the potential rate. In our simulations, h_{crit} was assumed to be −10 000 cm (we found that the results were not sensitive to this parameter value). The actual transpiration rate is determined by the model by integrating Equation (4) over the rooting depth.

To specify the potential transpiration (T_p) and evaporation (E_p) rates, potential evapotranspiration ($\mathrm{ET_p}$) was first calculated according to the Penman-Moneith equation (Liu *et al.*, 2005):

$$\mathrm{ET_p} = \frac{\Delta(R_{\mathrm{n}} - G) + \rho_a c_p (e_{\mathrm{s}} - e_a)/r_a}{\lambda \rho_{\mathrm{w}} \left[\Delta + \gamma\left(1 + \dfrac{r_{\mathrm{s}}}{r_a}\right)\right]} \tag{6}$$

where Δ is the slope of the saturation vapour pressure curve (kPa °C^{-1}); R_{n} is the net radiation (MJ m^{-2}); G is the soil heat flux (MJ m^{-2}); ρ_a is the air density (kg m^{-3}); ρ_{w} is the water density (kg m^{-3}); e_{s} is the saturation vapour pressure (kPa); e_a is the actual vapour pressure (kPa); c_p is the heat capacity of moist air (MJ kg^{-1} °C^{-1}); and r_{s} is the surface resistance (s m^{-1}), calculated for trees according to formulae given by Rey (1999) and Kelliher *et al.* (1993); γ is the psychrometre constant (kPa °C^{-1}); λ is the latent heat of vaporization (MJ kg^{-1}); and r_a is the aerodynamic resistance for heat and vapour transfer (s m^{-1}), calculated according to the method of Thom (1972) using the plant height and branch growth data.

Potential evaporation E_{p} was then calculated according to the following equation:

$$\begin{aligned} E_{\mathrm{p}} &= \mathrm{veg_{max}} \times T_{\mathrm{p}} \times \exp(-0{\cdot}623\mathrm{LAI}) \\ &\quad + \mathrm{ET_p} \times (1 - \mathrm{veg_{max}}) \end{aligned} \tag{7}$$

where $\mathrm{veg_{max}}$ (<1) is the maximum fraction of *P. euphratica* cover and LAI is the leaf area index. Equation (7) is a modification of an expression given by Al-Khafaf *et al.* (1978), formulated to account for the fact that the *P. euphratica* surface coverage was less than 100%. Values for $\mathrm{veg_{max}}$ and LAI were determined from the field measurements described above. The potential transpiration rate was then given by the following equation:

$$T_{\mathrm{p}} = \mathrm{ET_p} - E_{\mathrm{p}} \tag{8}$$

The daily potential evaporation and transpiration values used in the model surface boundary condition are shown in Figure 3. Also shown is the mean daily air temperature.

The lower boundary was specified as a time-varying pressure head boundary condition for simulations with

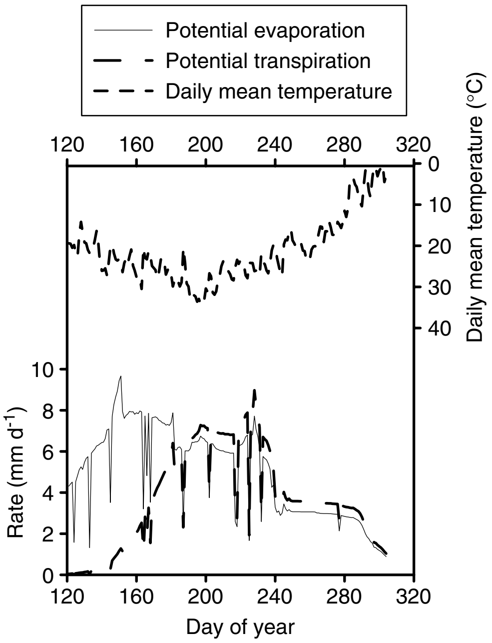

Figure 3. Potential evaporation and transpiration rates and daily mean temperature

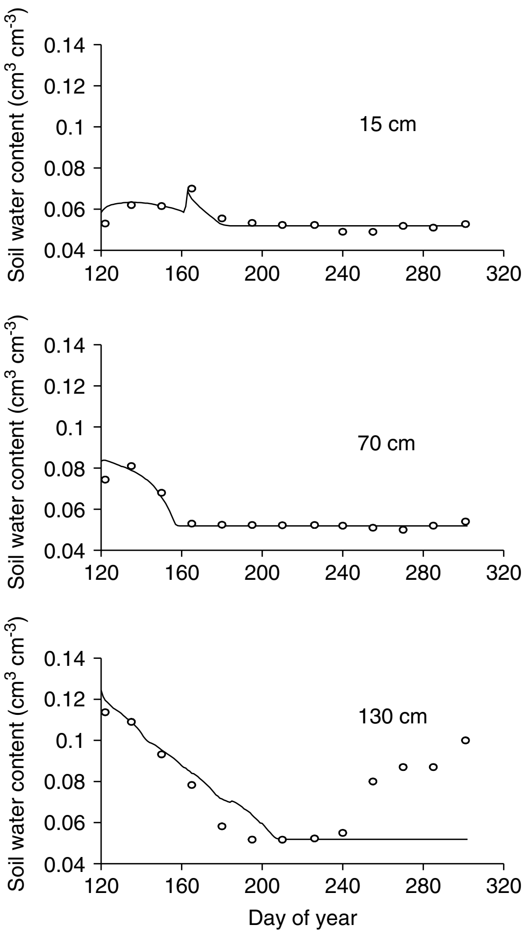

Figure 4. Comparison of simulated and measured soil moisture contents at the 15 cm, 70 cm and 130 cm depths during the *P. euphratica* growth period (May 1 through October 31)

a time-varying water table condition, and as a constant pressure head condition for constant water table conditions. The initial soil moisture profile was specified based on soil moisture data collected at the beginning of the simulation period.

Soil hydraulic parameters. As noted previously, the soil at the experimental site had a bulk density of 1·4 g cm^{-3} and was 91·2% sand, 4·8% silt and 4% Clay (Feng and Chen, 1999). Values for the soil hydraulic parameters were estimated by inputting this bulk density and texture data into the Rosetta pedotransfer function model (Schaap *et al*., 2001) that is part of the HYDRUS-1D package. The estimated van Genuchten-Mualem parameters were as follows: $K_s = 522{\cdot}01$ cm day^{-1}, $\theta_r = 0{\cdot}0517$ cm^{-3} cm^{-3}, $\theta_s = 0{\cdot}4194$ cm^{-3} cm^{-3}, $\alpha_{vg} = 0{\cdot}035$ cm^{-1}, $n = 2{\cdot}6787$ and $l = 0{\cdot}5$.

Root distribution. The data for the *P. euphratica* root distribution indicated that 10% of the active root length was located in the top 60 cm of soil, 60% was located between 60 and 100 cm, 25% between 100 and 180 cm and 5% between 180 and 200 cm. Consistent with this data, we model the root distribution with the following normalized function:

$$R(z) = \begin{cases} 9/L_R & 0 \le z \le 60 \text{ cm} \\ 81/L_R & 60 < z \le 100 \text{ cm} \\ 16{\cdot}875/L_R & 100 < z \le 180 \text{ cm} \\ 13{\cdot}5/L_R & 180 < z \le 200 \text{ cm} \end{cases} \quad (9)$$

where $z = 0$ cm is the soil surface, $z = 200$ cm is the maximum rooting depth and $L_R = 5400$ cm is the measured total length of roots.

RESULTS

HYDRUS-1D calibration

Figure 4 shows the results of the calibration exercise in which values for the drought stress parameters h_{50} and p were evaluated. In this exercise, h_{50} and p were varied and resulting simulated soil moisture contents were compared with measured data. Data for only selected representative depths are shown: A near-surface depth (15 cm), a middle depth where the root density was high (70 cm) and a deeper depth where the root density was lower (130 cm). As expected for such a coarse soil (see above), the simulated water contents in Figure 4 were not very sensitive to the uptake reduction parameters; the results shown in Figure 4, computed with $h_{50} = -950$ cm and $p = 3$, changed only slightly when these parameters were varied over the range of values reported in the literature. Nevertheless, even though the soil's steep water retention curve caused the drought stress function to operate in a step-like fashion, the simulations were in relatively good agreement with the measured water content data.

Table I gives the root mean square error and the relative mean error for the simulations and data presented in Figure 4. The agreement between the simulation and the data is very good at the 15 cm and 70 cm depths, and

DOI: 10.1002/hyp

Table I. Goodness of fit measures for Figure 4

Depth (cm)	Root mean square error (cm^3 cm^{-3})	Average relative error
15	0·0026	−0·0058
70	0·0021	0·0001
130	0·0204	−0·0792

is very good at the 130 cm depth for the first 100 days or so. However, starting at about day of year (DOY) 235, the data and simulation diverge: The simulated water content remains low while the measured water content increases. The reason for this discrepancy is not known at this time. Given the lack of precipitation after DOY 235 (Figure 2) and the non-increasing soil water content at the shallower depths, the measured increase in water content at 130 cm was presumably due to water entering the root zone from below. The groundwater level at the site is affected by the flow in the lower Heihe, which in turn is affected by seasonal variations and by water management in the upper and middle Heihe. The groundwater elevation data in Figure 2 show a sharp increase in the water table elevation, but not until about DOY 290. It is possible that there was an earlier rise in the water table at the site that was for some reason not indicated in our observation well, which was located about 40 m outside the study area. Simulations with a fictitious water table elevation that increased sharply at about DOY 235 produced a simulated water content at 130 cm that increased similarly to the measured data.

Figure 4 illustrates the importance of groundwater to the survival of the *P. euphratica* woodland. Although several rainfall events occurred during the study period (Figure 2), only in one instance was the precipitation sufficient to increase soil moisture at even the 15 cm depth, and then the increase was almost negligibly small. Clearly, a substantial portion of the water consumed by the plant during the study must have come from groundwater.

Groundwater contribution to root zone soil moisture

To further investigate the impact of groundwater on *P. euphratica* root zone soil moisture, we performed a series of simulations with constant groundwater depths of 2, 2·5 and 3 m. In these simulations, all conditions except the groundwater level were the same as those used in the above model calibration (e.g. surface boundary conditions based on field measurements).

Figure 5 shows for each scenario the computed total root water uptake and the computed water flux at the bottom of the root zone, $z = 200$ cm (we modified the HYDRUS-1D source code to compute and output this latter flux). The high frequency fluctuations in the computed root zone water flux for the time-varying water table case are artefacts introduced by the time discretization of the bottom boundary condition (i.e. the water table elevation). The bottom boundary condition was discretized in daily steps, meaning changes in water table elevation occur (essentially) instantaneously at the start of a new day. Such an abrupt change in boundary pressure requires a large spike in the boundary flux.

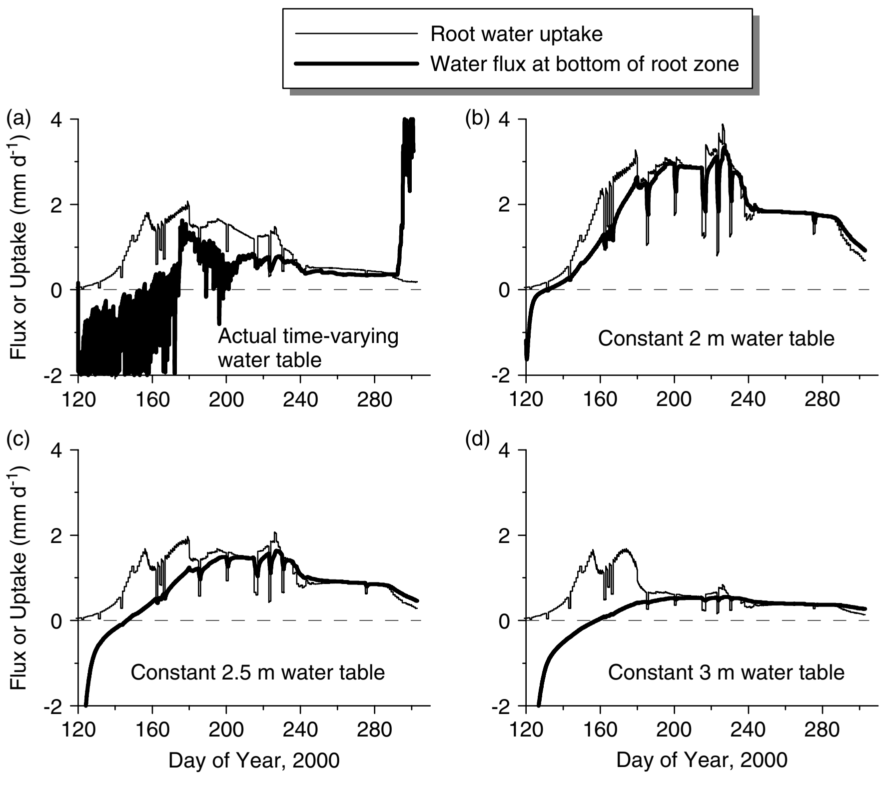

Figure 5. The simulated root water uptake and water flux at the bottom of the root zone ($z = 2$ m) for different water table depths. Negative water flux values indicate drainage from the root zone to the deeper soil or groundwater, whereas positive values indicate upwards flow into the root zone

DOI: 10.1002/hyp

Those spikes affect the lower root zone water flux, particularly in the early part of the growing season when the water table extended from the boundary to just below the root zone. However, because of the time scale, the plot is somewhat misleading regarding the nature of the fluctuations—they are actually brief departures from a relatively smoothly varying curve, but that level detail is not visible in the plot.

Overall, the plots in Figure 5 show that drainage from the root zone (shown as a negative flux) occurred initially, particularly in the 2·5 and 3 m water table scenarios. The drainage occurred because each simulation used as an initial condition the initial soil moisture profile for the actual case, which included saturated soil conditions starting at about the 2 m depth (see, Figure 2) and a relatively high root zone soil moisture content. Obviously, that initial condition was not in equilibrium with the deeper water table scenarios, and hence the initial drainage. The drainage lasted about 20–30 days, after which time, the simulations were no longer affected by the initial conditions. At subsequent times, Figure 5 indicates an upwards (positive) water flux into the soil profile that, as expected, decreases with increasing water table depth. As the growing season progresses, the root water uptake and bottom root zone water flux are nearly equal.

Figure 6 shows the simulated cumulative water fluxes at the bottom of the root zone as well as the cumulative root water uptake. Note that the curves in Figure 6 correspond to the area under the curves in Figure 5. However, the cumulative totals in Figure 6 exclude the first 40 days of the simulation shown in Figure 5, thereby negating the impact of the initial conditions. Figure 6 permits a quantitative assessment of the seasonal contributions of groundwater to root zone soil moisture and plant uptake as affected by groundwater depth. Consider first the cumulative water flux results. With a constant groundwater depth of 2 m, approximately 300 mm of groundwater moved up into the root zone. When the constant groundwater depth was increased to 2·5 m, the groundwater contribution decreased to about 150 mm, whereas for a 3 m depth, the contribution was about 60 mm. The actual time-varying water table scenario, with an average water table depth of 2·64 m, produced a groundwater contribution to root zone moisture that was intermediate to the other cases (approximately 115 mm), with a significant portion of that contribution occurring at the very end of the growing season when the water table was rising and uptake/transpiration was low (Figures 2 and 3).

The simulated cumulative root water uptake totals shown in Figure 6 follow a similar pattern for each of the three constant water tables. As was visible in Figure 5, in these three cases, the water uptake initially exceeded the lower root zone flux as the tree-utilized water already present in the root zone, and thus the cumulative uptake initially grows faster than the cumulative flux. But by about DOY 200, the plant was using water originating from below the root zone, the uptake rate and lower root zone flux were approximately equal and thus the cumulative curves grow identically during this period. The actual time-varying case had a slightly different dynamic in that the gap between the two curves (cumulative uptake and root zone flux) grew wider over a longer period of time before they began to mirror on another. Additionally, in the final days of the simulation, the increase in water table elevation resulted in a sharp increase in the lower root zone flux, but the transpiration demand was low at that time and thus the water replenished the root zone but was not consumed in significant amounts by the tree.

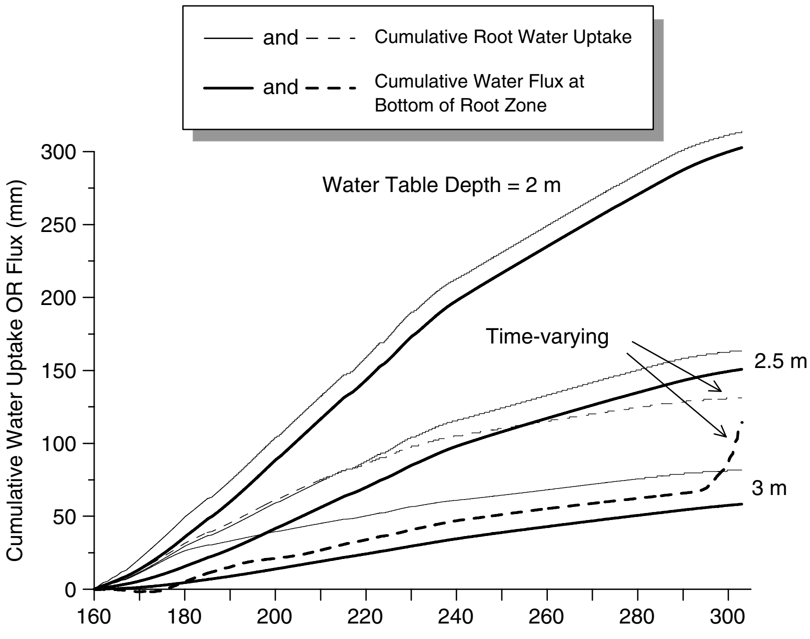

Figure 6. Cumulative water flux at the bottom of the root zone and cumulative root water uptake, starting from day of year 160

DOI: 10.1002/hyp

The simulated seasonal totals for water uptake are relatively low, about 160 mm for the actual time-varying case. The cumulative potential transpiration total during the whole season was considerably bigger, about 675 mm. We note, however, that the computed uptake values are comparable to annual transpiration amounts that have been observed in other deciduous woodlands (e.g. Ffolliott *et al*., 2003; Pataki and Oren, 2003).

The findings for groundwater contributions to transpiration are summarized in Table II. We considered only the time period DOY 160–290 for these totals. Focusing on this period eliminates any effects that the initial water content distribution may have had on the groundwater flux, and also eliminates in the time-varying case the large water flux at the end of the season that replenished the root zone moisture but was not used by the tree. During the considered time period, to a good approximation, all groundwater entering the root zone was utilized by the plant, and thus the ratio of the cumulative groundwater flux to the cumulative root uptake is approximately equal to the fraction of groundwater in the transpired water. The results in Table II show that increasing the water table depth from 2 to 2·5 m reduced transpiration (uptake) by about half, from 301 mm to 158 mm. The groundwater contribution was very high in both cases, 95% for the 2 m case and 90% for the 2·5 m case. Increasing the water table depth to 3 m halved again the transpiration total (79 mm), and also reduced on a percentage basis the groundwater contribution (68%). In the time-varying case, the groundwater contribution to the 125 mm of transpiration was lower, 53%. Note, however, that this total would likely be higher if we could have considered a longer time period. A large percentage of the water consumed in the early and early mid parts of the growing season probably originated from groundwater, but in our analysis that water was part of the 'initial condition' and thus did not count as groundwater in our calculations.

Previous field investigations (Chen *et al*., 2004; Wang *et al*., 2007) of *P. euphratica* in the Tarim River watershed, China, indicated that the optimal groundwater water depth was in the approximate range of 3 to 4 m, with non-stressed conditions found at 3·82 m, mild stress at 4·74 m and moderate stress at 5·82 m. Additionally, certain physiological indicators of *P. euphratica* stress (namely, proline accumulation in tissues) increased when the water table depth was shallower than approximately 3 m; this stress was partially attributed to increases in groundwater salinity that accompanied the elevated water table conditions (Chen *et al*., 2004; Wang *et al*., 2007). Other possible problems associated with overly shallow groundwater include an increased potential for root disease and a higher likelihood of root damage during winter freezes (Liu *et al*., 2007).

Table II. Cumulative totals for simulated transpiration and groundwater fluxes during the middle part of the growing season (day of year 160–290)

Water table depth (m)	Transpiration (mm)	Groundwater flux (mm)	Approximate percentage of transpiration derived from groundwater
Time varying	125	66	53
2	301	287	95
2.5	158	143	90
3	79	54	68

Our simulations of *P. euphratica* stress as a function of groundwater depth for a site near the Heihe River are not consistent with the field observations made at the Tarim River. However, the response of *P. euphratica* to groundwater depth and other hydrologic parameters probably depends on factors that vary from region to region. For example, Liu *et al*. (2007) found the hydrologic response of *P. euphratica* in the Heihe River basin to be different from that observed in the Tarim River area, finding a negative correlation between Heihe River runoff and *P. euphratica* growth instead of the positive correlation reported previously for the Tarim River. Liu *et al*. (2007) posited that the optimal water table depth at their Heihe site was in the range of 2–4 m.

More generally, the ideal water table height is expected to depend on soil type, with finer textured soils providing greater capillary rise but also being more susceptible to salinity, waterlogging and associated root disease and damage. Also, sites may vary in terms of the rooting development as affected by the age of the trees and the historical conditions under which the trees developed. For example, at one oasis in the Taklamakan desert, it was observed that an older stand of *P. euphratica* was able to use groundwater as deep as 24 m, likely because the strand originated in a lowland dune that gradually grew in elevation (Gries *et al*., 2003). Our site in the Heihe watershed featured a very coarse soil texture (91% sand) and 10-year-old trees with a relatively shallow rooting depth, and consequently would likely benefit from water tables as shallow as 2 m. One advantage of the modelling methodology used in this study is that by re-running the simulations using different values for soil-specific parameters such as the hydraulic parameters in Equations (2) and (3), it is easy to compare results for differing soil environments.

SUMMARY AND CONCLUSIONS

In this work, we investigated the uptake of groundwater by *P. euphratica* in a 10-year-old riparian woodland in an arid region of Northwest China. Analyses were performed using a combination of field measurements and simulations of root zone water flow and uptake processes performed with the HYDRUS-1D software package. The conclusions are as follows:

1. HYDRUS-1D simulations of the *P. euphratica* root zone during its growing period from 1st May to 30th October, 2000, resulted in simulated soil moisture contents that were in good agreement with moisture contents measured in the field. The simulated processes

DOI: 10.1002/hyp

included root water uptake and groundwater flow into the root zone. It was judged that the HYDRUS-1D model could be used to simulate uptake processes for individual representative trees in arid areas of Northwest China.

2. Using model simulations, the impact of the water table depth on *P. euphratica* water uptake was investigated. Simulations made using the actual time-varying water table depth (average depth of 2·64 m) as the lower boundary condition indicated that *P. euphratica* transpiration during the middle part of the growing season (DOY 160–290) was 125 mm, with 66 mm of that water coming from groundwater (53%). Simulations for constant water table depths found that increasing the water table depth from 2 to 3 m resulted in a 74% reduction in transpiration. For simulations with water tables between 2 and 2·5 m, more than 90% of the transpired water originated from groundwater.
3. In assessing the impact of water table depth on *P. euphratica* water use, and by extension the impact of Ejina Basin water management on *P. euphratica* survival, there are many factors to consider, including soil texture, soil heterogeneity and the age of the woodland and extent of root development. Thus, the optimal water table depth, or optimal range of water table depths, is likely to vary from location to location. An advantage of the modelling approach is that these and other factors can be systematically varied, creating a site-specific impact assessment of water management option that may alter water table depths, thus aiding ecological restoration efforts.

ACKNOWLEDGEMENT

This research is supported by National Basic Research Program of China (2006CB400502); supported by the 111 Project under Grant No. B08048, Ministry of Education and State Administration of Foreign Experts Affairs, China; supported by the Program for Changjiang Scholars and Innovative Research Team in University under Grant No. IRT0717, Ministry of Education, China; and also supported by the Grand Sci-Tech Research Project of Ministry of Education under Grant No. 308012. The authors are grateful to soil physical scientist van Genuchten, M. Th. His suggestions have contributed significantly to the improvement of the manuscript. The authors are grateful to the reviewers; the comments and suggestions of the reviewers have contributed significantly to the improvement of the manuscript.

REFERENCES

Al-Khafaf S, Wierenga PJ, Williams BC. 1978. Evaporative flux from irrigated cotton as related to leaf area index, soil water and evaporative demand. *Agronomy Journal* **70**: 912–917.

Ayars JE, Schoneman RA. 1986. Use of saline water from a shallow water table by cotton. *Transactions of the ASAE* **29**: 1674–1678.

Babajimopoulos C, Budina A, Goukos D. 1995. SWBACROS: A model for the estimation of the water balance of a cropped soil. *Environmental Software* **10**(3): 211–220.

Babajimopoulos C, Panoras A, Georgoussis H, Arampatzis G, Hatzigiannakis E, Papamichail D. 2007. Contribution to irrigation from shallow water table under field conditions. *Agricultural Water Management* **92**: 205–210.

Bai F, Li WP, Li ZH. 2008. Analysis on the main causes resulting in vegetation degeneration in the Heihe River Basin. *Arid Zone Research* **25**(2): 219–224.

Cao W, Wan L, Zhou X, Hu F, Chen J, Gong B, Zhang W, Dong Y. 2004. Effects of variation in water environment on ecosystem in the lower reaches of the Heihe watershed. *Hydrogeology and Engineering Geology* **31**: 21–25.

Chen YN, Wang Q, Ruan X, Li WH, Chen YP. 2004. Physiological response of *Populus euphratica* to artificial water-recharge of the lower reaches of Tarim River. *Acta Botanica Sinica* **46**: 1393–1401.

Chen Y, Zhang D, Sun Y, Liu X, Wang N, Savenije HHG. 2005. Water demand management: a case study of the Heihe River basin in China. *Physics and Chemistry of the Earth* **30**: 408–419.

Chen YP, Chen YN, Li WH, Xu CC. 2006b. Characterization of photosynthesis of *Populus euphratica* grown in the arid region. *Photosynthetica* **44**: 622–626.

Du Q, Xu X, Li H, Peng H. 2005. Analysis on ecological security changes of the oases in the middle and lower Heihe River. *Acta Scientiarum Naturalium Universitatis Pekinensis* **41**(2): 273–281.

Feng Q, Chen G. 1999. Moisture distribution and movement in sandy lands of China. *Acta Pedologica Sinica* **36**(2): 225–236.

Ffolliott PF, Gottfried GJ, Cohen Y, Schiller G. 2003. Transpiration by dryland oaks: studies in the south-western United States and Northern Israel. *Journal of Arid Environments* **55**: 595–605.

Gries D, Zeng F, Foetzki A, Arndt SK, Bruelheide H, Thomas FM, Zhand X, Runge M. 2003. Growth and water relations of *Tamarix ramosissima* and *Populus euphratica* on Taklamakan desert dunes in relation to depth to a permanent water table. *Plant Cell and Environment* **26**: 725–736.

Gu R, Liu Q, Pei D, Jiang X. 2004. Understanding saline and osmotic tolerance of *Populus euphratica* suspended cells. *Plant Cell Tissue and Organ Culture* **78**: 261–265.

He Z, Zhao W. 2006. Characterizing the spatial structures of riparian plant communities in the lower reaches of the Heihe River in China using geostatistical techniques. *Ecological Research* **21**: 551–559.

Kahlown MA, Ashraf M, Zia-ul-Haq. 2005. Effect of shallow groundwater table on crop water requirements and crop yield. *Agricultural Water Management* **76**(1): 24–35.

Kelliher FM, Leuning R, Schulze E-D. 1993. Evaporation and canopy characteristics of coniferous forests and grasslands. *Oecologia* **95**: 153–163.

Liu S, Graham WD, Jacobs JM. 2005. Daily potential evapotranspiration and diurnal climate forcings: influence on the numerical modeling of soil water dynamics and evapotranspiration. *Journal of Hydrology* **309**: 39–52.

Liu P-X, Peng J-F, Chen F-H. 2007. Hydrological response of *Populus euphratica* Olve. radial growth in Ejinaa Banner, Inner Mongolia. *Journal of Integrative Plant Biology* **49**: 150–156.

Lu J, Zhong S, Li L, Pan S. 2007. *Analysis of ecological restoration of inland desert oasis based on remote sensing*. Available online at http://www.digitwater.net/articleinfo.asp?ID=113.

Pataki DE, Oren R. 2003. Species differences in stomatal control of water loss at the canopy scale in a mature bottomland deciduous forest. *Advances in Water Resources* **26**: 1267–1278.

Qi S, Cai Y. 2007. Mapping and assessment of degraded land in the Heihe River basin, Arid Northwestern China. *Sensors* **7**: 2565–2578.

Qi S, Luo F. 2007. Environmental degradation problems in the Heihe River basin, northwest China. *Water and Environment Journal* **21**: 142–148.

Rey JM. 1999. Modelling potential evapotranspiration of potential vegetation. *Ecological Modelling* **123**: 141–159.

Schaap MG, Leij FJ, van Genuchten MTh. 2001. ROSETTA: A computer program for estimating soil hydraulic properties with hierarchical pedotransfer functions. *Journal of Hydrology* **251**: 163–176.

Si J-H, Feng Q, Zhang X-Y, Su Y-H, Zhang Y-W. 2005. Vegetation changes in the lower reaches of the Heihe River after its water import. *Acta Botanica Boreali-Occidentalia Sinica* **25**: 631–640.

Šimůnek J, van Genuchten MTH, Šejna M. 2005. *The HYDRUS-1D Software Package for Simulating the Movement of Water, Heat, and Multiple Solutes in Variably Saturated Media*, *HYDRUS Software Series No. 1*, Version 3·0. Department of Environmental Sciences, University of California Riverside: Riverside, California USA.

Skaggs TH, Shouse PJ, Poss JA. 2006a. Irrigating forage crops with saline waters: 2. Modeling root uptake and drainage. *Vadose Zone Journal* **5**: 824–837.

Skaggs TH, van Genuchten MTh, Shouse PJ, Poss JA. 2006b. Macroscopic approaches to root water uptake as a function of water and salinity stress. *Agricultural Water Management* **86**: 140–149.

Soppe RWO, Ayars JE. 2003. Characterizing groundwater use by safflower using lysimeters. *Agricultural Water Management* **60**: 59–71.

Thom AS. 1972. Momentum, mass and heat exchange of vegetation. *Quarterly Journal of the Royal Meteorological Society* **98**: 124–134.

van Genuchten MTh. 1987. *A numerical model for water and solute movement in and below the root zone*. Unpublished Research Report, U.S. Salinity Laboratory, USDA, ARS, Riverside, CA.

Wang G, Chen G. 1999. Water resource development and its influence on the environment in arid areas of China—the case of the Hei River basin. *Journal of Arid Environment* **43**: 121–131.

Wang Q, Ruan X, Chen YN, Li WH. 2007. Eco-physiological response of *Populus euphratica* Oliv. to water release of the lower reaches of the Tarim River, China. *Environmental Geology* **53**: 349–357.

Xu Z, Cheng G, Zhang Z, Su Z, Loomis J. 2003. Applying contingent valuation in China to measure the total economic value of restoring ecosystem services in Ejina region. *Ecological Economics* **44**: 345–358.

Yang Y, Wang W, Ottow EA, Polle A, Zhang F, Lan H, Jiang X. 2007. The physiological mechanism of *Populus euphratica* adapting to drought stress. *Electronic Journal of Biology* **3**: 56–60.

Yan D, Wang H, Qin D, Wang J, Li Y. 2005. The ecological evolution driven by water in the lower reaches of Heihe Basin, China. *Environmental Science* **25**(1): 37–41, (In Chinese).

Zhu Y. 2002. *The study of water transfer laws in groundwater-soil-plant-atmosphere continuum in arid areas in Northwest China*. PhD thesis, Cold and Arid Regions Environmental and Engineering Research Institute, CAS, Lanzhou, Gansu, China.

Zhu Y, Wu Y. 2003. Water consumption of natural plant *Alhagi sparsifolia* in arid desert region. *Bulletin of Soil and Water Conservation* **23**(4): 43–45.

Zhuang L, Chen YN. 2006. Physiological responses of three contrasting plant species to groundwater level changes in an arid environment. *Journal of Integrative Plant Biology* **48**: 520–526.

DOI: 10.1002/hyp